Neuron
Article

Cell PRESS

Interaction between Reelin and Notch Signaling Regulates Neuronal Migration in the Cerebral Cortex

Kazue Hashimoto-Torii,[1,2] Masaaki Torii,[1,2,3,4] Matthew R. Sarkisian,[1,2] Christopher M. Bartley,[1,2] Jie Shen,[5] Freddy Radtke,[6] Thomas Gridley,[7] Nenad Šestan,[1,2] and Pasko Rakic[1,2,*]
[1]Department of Neurobiology
[2]Kavli Institute for Neuroscience
Yale Medical School, 333 Cedar Street, New Haven, CT 06510, USA
[3]Vanderbilt Kennedy Center for Research on Human Development
[4]Department of Pharmacology
Vanderbilt University, Nashville, TN 37203, USA
[5]Center for Neurologic Diseases, Brigham and Women's Hospital, Program in Neuroscience, Harvard Medical School, Boston, MA 02115, USA
[6]Ludwig Institute for Cancer Research, Chemin de Boveresses 155, CH-1066 Epalinges, Switzerland
[7]The Jackson Laboratory, 600 Main Street, Bar Harbor, ME 04609, USA
*Correspondence: pasko.rakic@yale.edu

SUMMARY

Neuronal migration is a fundamental component of brain development whose failure is associated with various neurological and psychiatric disorders. *Reelin* is essential for the stereotypical inside-out sequential lamination of the neocortex, but the molecular mechanisms of its action still remain unclear. Here we show that regulation of Notch activity plays an important part in Reelin-signal-dependent neuronal migration. We found that Reelin-deficient mice have reduced levels of the cleaved form of Notch intracellular domain (Notch ICD) and that loss of Notch signaling in migrating neurons results in migration and morphology defects. Further, overexpression of Notch ICD mitigates the laminar and morphological abnormalities of migrating neurons in *Reeler*. Finally, our in vitro biochemical studies show that Reelin signaling inhibits Notch ICD degradation via Dab1. Together, our results indicate that neuronal migration in the developing cerebral cortex requires a Reelin-Notch interaction.

INTRODUCTION

Cerebral cortical development is composed of multiple processes, including neuronal production from neuroepithelium, migration of neurons to their proper positions, and neuronal maturation (Rakic, 1988; Kriegstein and Noctor, 2004). These steps are tightly controlled by various molecular pathways (Caviness and Rakic, 1978; Walsh and Goffinet, 2000; Lambert de Rouvroit and Goffinet, 2001; Olson and Walsh, 2002; Bielas and Gleeson, 2004; LoTurco and Bai, 2006; Ayala et al., 2007; Kawauchi and Hoshino, 2008). For example, the precise positioning of radially

migrating neurons is critically controlled by the Reelin signaling pathway and is indispensable for forming a stereotypical inside-out, six-layered pattern (Bar et al., 2000; Magdaleno and Curran, 2001; Rice and Curran, 2001; Tissir and Goffinet, 2003; Soriano and Del Rio, 2005; Kanatani et al., 2005; Forster et al., 2006; D'Arcangelo, 2006).

Reelin deficiency (*Reeler*) is characterized by an inverted lamination of the neocortex, and the human *Reelin* (*RELN*) mutation has been linked to lissencephaly, autism, and other disorders (Hong et al., 2000; Zaki et al., 2007). Reelin encodes an extracellular matrix-associated glycoprotein that is secreted by Cajal-Retzius cells in the developing cerebral cortex. Very low density lipoprotein receptor (Vldlr) and apolipoprotein E receptor type2 (ApoER2) are canonical Reelin-binding receptors that subsequently activate intracellular Dab1 (Sheldon et al., 1997; Howell et al., 1997, 1999, 2000; Ware et al., 1997; Rice et al., 1998; Trommsdorff et al., 1999; Hiesberger et al., 1999; D'Arcangelo et al., 1999) and mediate divergent roles in neuronal migration (Hack et al., 2007). Dab1 interacts with multiple molecules, but most of these interactions have yet to be examined formally in migrating neurons (Bock et al., 2003; Ballif et al., 2004; Suetsugu et al., 2004; Chen et al., 2004; Pramatarova et al., 2003, 2008; Jossin and Goffinet, 2007). Thus the underlying molecular mechanisms of Reelin signaling that contribute to *Reeler* pathogenesis remain elusive.

Notch signaling represents another molecular pathway that is integral to cortical development. Delta and Serrate (known as Jagged in mammals) ligand binding to Notch receptors causes proteolytic release of the Notch ICD, the active form of Notch, which translocates to the nucleus and induces transcription of multiple target genes by forming a transcriptional complex with Rbpj (also known as CBF-1), a transcriptional factor that mediates canonical Notch signaling. This pathway has well-characterized roles in neurogenesis including cell elimination by controlling apoptosis and dendrite morphogenesis (reviewed by Yoon and Gaiano, 2005; Louvi and Artavanis-Tsakonas, 2006).

Previous studies have shown that Notch1 protein strongly localizes in the nuclei of cortical neurons as they accumulate beneath the marginal zone (MZ) (Šestan et al., 1999; Redmond et al., 2000), which consists of Reelin-expressing Cajal-Retzius cells. Although a *Reelin* homolog has not been identified in invertebrates including *Drosophila*, it also has been shown that Disabled (a *Drosophila* homolog of mammalian Dab1) binds Notch in vitro (Giniger, 1998; Le Gall and Giniger, 2004; Le Gall et al., 2008). Furthermore, reduction of a Notch downstream gene has been reported in *Reeler* mutant mice (Baba et al., 2006). These observations led us to hypothesize that Notch may play a role in Reelin-regulated lamination of the mammalian neocortex. In the present study, we provide evidence for a Reelin and Notch signaling pathway interaction that regulates neuronal migration during cerebral cortical development.

RESULTS

Notch Activity in Migrating Neurons Is Reduced in *Reeler* Cerebral Cortex

To test our hypothesis, we first used immunostaining to examine whether the expression pattern of Notch1 is altered in *Reelin*-deficient cortex during the peak period of radial migration to layers II and III of the developing cortical plate (CP). Using an antibody targeted against the Notch1 ICD, we observed strong expression of Notch1 in the nuclei of wild-type cortical neurons beneath the MZ as previously reported (Šestan et al., 1999; Redmond et al., 2000), which gradually became weaker toward lower layers and the intermediate zone (IZ) (Figures 1A and 1A′). Strikingly, nuclear Notch1 expression is severely reduced in *Reeler* (*rl/rl* in Figures 1C and 1C′). Upon stimulation by its ligands, the Notch receptor undergoes several cleavages to become its activated form, which translocates to the nucleus. Since the Notch1 antibody recognizes the intracellular domain of both cleaved (active) and uncleaved (nonactive) forms of Notch1 gene products, nuclear Notch1 label presumably represents cleaved Notch1 ICD. In contrast, cytoplasmic expression of Notch1 in *Reeler* appeared to be comparable to that in wild-type (Figures 1A–1D′). To confirm the reduction of Notch1 ICD in *Reeler* cortex, we performed immunostaining using a different antibody that specifically recognizes the Notch1 ICD form. The presence of nuclear Notch1 ICD was strong in the cortex of wild-type mice, but dramatically reduced in *Reeler* mice (Figures 1E–1F′). Reduced Notch1 ICD was also observed in the *Vldlr/ApoER2* Reelin signaling receptors double knockout (dKO) (Figures 1G and 1H) and the signaling mediator *Dab1* knockout (*Scrambler*) (data not shown).

To confirm our immunohistochemistry, we probed protein extracts from *Reeler* neocortex with each of the Notch1 antibodies. We observed an ~50% decrease in Notch1 ICD, but no significant difference in the full-length (Figure 1I) and membrane-anchored transient intermediate forms of Notch1 (Figure S1, available online). Similar results were obtained from the *Vldlr/ApoER2* dKO and *Dab1* knockout neocortex (data not shown). Previous studies have shown that inhibition of S1 or S2-3 cleavage of Notch results in accumulation of full-length or transient intermediate Notch proteins, respectively. The evidence that no significant increases in full-length or transient Notch1 precursors were observed in *Reeler* (Figure 1I and S1)
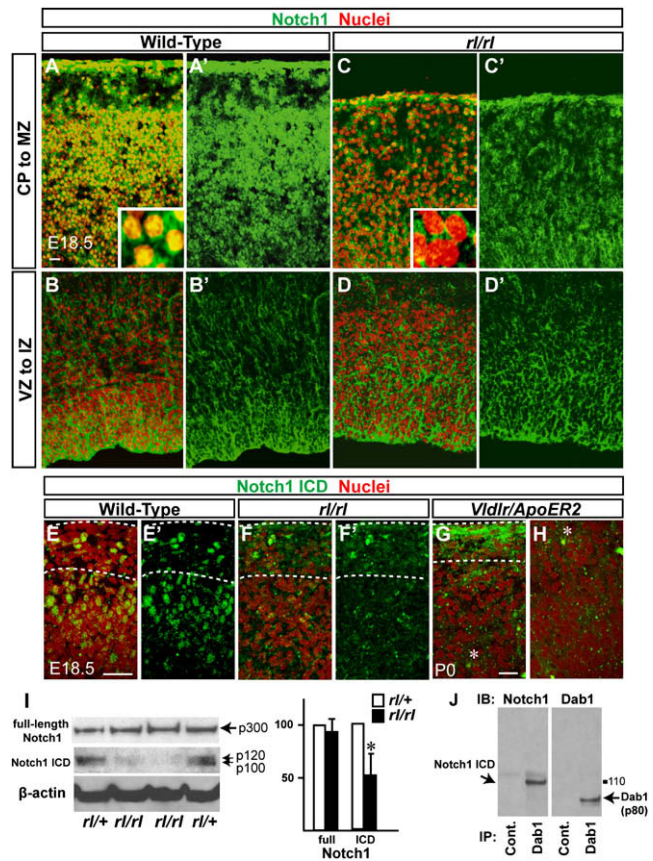
Figure 1. Nuclear Notch ICD Is Reduced in Cortical Neurons in *Reeler*

(A–H) Nuclei (red), Notch1 (green in [A]–[D′], antigen is Notch1 ICD), and Notch1 ICD cleaved form (green in [E]–[H]) immunostaining in the cortex of wild-type mice and mutants as indicated. Higher-magnifications are shown in the insets. Dashed lines in (E)–(G) indicate the pial surface and the border between CP and MZ in wild-type or superplate (SPP) in the mutants. (G) and (H) show upper CP and lower CP/IZ, respectively (the asterisk indicates the same cell). Note that Notch1 ICD expression at the lower CP (inverted layer II/III) is significantly decreased in *Vldlr/ApoER2* mutant (H), which is similar to *Reeler* (not shown). Green staining at the pial surface in (G) is nonspecific. Bars = 25 μm.

(I) Immunoblots of full-length Notch1 (p300), Notch1 ICD, and β-actin from the same cortical lysates of two *rl/+* and two *rl/rl*. Notch1 ICD bands include p110 nonphosphorylated and p120 phosphorylated forms. (Right) Relative values of the band intensity of indicated proteins from *rl/rl* against those from *rl/+,* which were set as 100. Band intensities for each mutant were normalized to β-actin. The data represent the mean ± SD of five brains from independent experiments. *p < 0.01 by paired t test.

(J) Immunoprecipitation (IP) of brain lysates with a nonspecific goat IgG as negative control (left) or Dab1-specific antibody (E-19; right) followed by Notch1 and Dab1 immunoblotting (IB).

suggests that Reelin signaling does not affect the proteolytic processing of the Notch receptor during cortical development. Therefore, the loss of Notch1 ICD in *Reeler* is likely due to other mechanisms, such as enhanced degradation, that would prevent Notch1 ICD from accumulating in the nucleus.

We next examined Notch activity in migrating neurons using Notch signaling-dependent reporter constructs. In utero

electroporation of the Rbpj-bp reporter construct enabled us to monitor the acute on/off level of Rbpj-dependent transcription activated by Notch signaling (Kohyama et al., 2005). The reporter expression confirmed Notch activity in postmitotic migrating neurons in both the IZ and CP in wild-type, as well as in mitotic neuronal progenitor cells in the ventricular zone/subventricular zone (VZ/SVZ) as previously reported (Kohyama et al., 2005; Ohtsuka et al., 2006; Figure S2). In contrast, the reporter activity was barely detected in *Reeler* (Figure S3).

These results suggest that Notch signaling is active in migrating neurons but is significantly reduced in Reelin-signaling-deficient cortex. As additional confirmation we performed quantitative RT-PCR and found that *Hes1* and *Hes5* (downstream target genes of Notch signaling) had reduced transcription in *Reeler* while the transcription level of *Notch1* was comparable to that of wild-type (Figure S3). Taken together, these findings suggest that Reelin signaling via Dab1 may regulate nuclear Notch ICD levels, and thereby active Notch signaling by mechanisms distinct from transcriptional regulation or cleavage processing of the Notch receptor.

Notch ICD and Dab1 Interact during Cerebral Cortical Development

We next tested whether the Reelin and Notch signaling pathways interact during cortical development. Using multiple antibodies against Dab1 (see antibody list in Supplemental Experimental Procedures), we were able to coimmunoprecipitate p110, a nonphosphorylated form (Redmond et al., 2000) of Notch1 ICD from E18.5 neocortical lysate (Figure 1J). Conversely, Dab1 coimmunoprecipitated with Notch1 when we used multiple antibodies against Notch1 ICD (data not shown; see antibody list in Supplemental Experimental Procedures). This is consistent with previous reports that *Drosophila* Disabled interacts with Notch via the phosphotyrosine-binding (PTB) domain (Giniger, 1998; Le Gall and Giniger, 2004) and that the Dab1 PTB domain preferentially binds nonphosphorylated proteins (Howell et al., 2000). These results indicate that Dab1 and Notch1 ICD physically interact during mouse cortical development and serve as the foundation for our hypothesis that a Reelin-Notch signaling interaction may be involved in neuronal migration in the cortex.

Notch Signaling Is Indispensable for Proper Radial Migration in the Cerebral Cortex

To test whether Notch signaling has a functional role in migration, we systematically deleted *Notch* genes within postmitotic migrating neurons. Because Notch also plays important developmental roles in Cajal-Retzius cells in the MZ and VZ/SVZ neural progenitor cells (Yoon and Gaiano, 2005; Louvi and Arta-vanis-Tsakonas, 2006), it was crucial to preclude any secondary effects of *Notch* deletion in these cell populations. We therefore took advantage of the Cre/loxP system in combination with in utero electroporation to delete *Notch* in postmitotic migrating neurons within the neocortex. As depicted in Figure 2A, we electroporated a construct including Cre recombinase and Venus (an enhanced yellow fluorescent protein [EYFP] variant) reporter under the T alpha 1 alpha-tubulin promoter (pTα1-Cre-IRES-Venus) into E14.5 cortex of *floxed Notch* mice. The Tα1 promoter activates predominantly in postmitotic neurons (Gloster et al.,
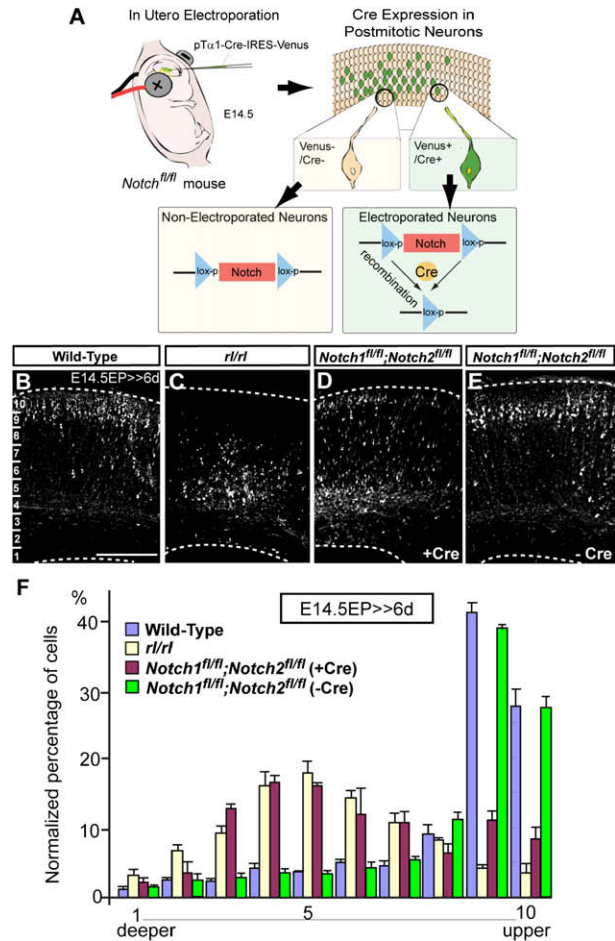
Figure 2. Notch Signaling Is Required for Proper Radial Migration of Cortical Neurons

(A) Schematic representation of *Notch* genomic deletion in the migrating neurons.

(B–E) Venus immunostaining 6 days postelectroporation with pTα1-Cre-IRES-Venus (B–D) or pTα1-IRES-Venus (E) into indicated mice. Bar = 100 μm. Dashed lines indicate pial and ventricular surfaces.

(F) The graph indicates quantification of the distribution of Venus⁺ neurons in the 10 bins dividing the whole thickness of the cortex as indicated in (B) in each genotype. The data represent the mean ± SEM of four brains each from independent experiments. p < 0.0001, p < 0.0001, and p > 0.05 for *rl/rl*, *Notch1^{fl/fl};Notch2^{fl/fl}*(+Cre), and *Notch1^{fl/fl};Notch2^{fl/fl}*(−Cre), respectively, compared with wild-type by two-sample Kolmogorov-Smirnov test (K-S test); $F_{(9,54)} = 107.40$, p < 0.0001; $F_{(9,45)} = 54.92$, p < 0.0001; and $F_{(9,54)} = 0.78$, p > 0.05, respectively, by repeated-measures ANOVA.

1994), allowing us to delete *Notch* in postmitotic neurons by Cre-mediated recombination (Figure 2A). Some reports claim that the Tα1 promoter also drives gene expression in a small population of mitotic neuronal progenitor cells (Sawamoto et al., 2001; Gal et al., 2006), while other groups detected expression only in postmitotic neurons (Gloster et al., 1994; Coksaygan et al., 2006). In our system, Cre/loxP recombination was activated almost exclusively in postmitotic neurons, which was confirmed by a series of experiments (Figure S4). In the Supplemental Data, we further discuss the differences between the

experimental systems used in our previous (Gal et al., 2006) and current report.

Deletion of *Notch1* by introduction of pTα1-Cre-IRES-Venus into *floxed Notch1* homozygote (*Notch1*^{fl/fl}) resulted in a distribution of Venus^{+} neurons in the cortex that was similar to that of wild-type, *floxed Notch1*, and *Notch2* (closest paralog of *Notch1*) heterozygotes (Figure S5 and data not shown). Similarly, *Notch2* deletion (*Notch2*^{fl/fl}) did not affect neuronal positioning (Figure S5). To eliminate possible compensatory effects of single *Notch* deletion, we next deleted *Notch1* and *Notch2* simultaneously. In contrast to wild-type cortex in which most Venus^{+} neurons reached the upper CP (Figures 2B and 2F), many Venus^{+} neurons in *Notch1*^{fl/fl}; *Notch2*^{fl/fl} brains were abnormally located within the lower CP and IZ (Figures 2D and 2F). Although direct comparison between the cases in *Reeler* (Figure 2C) and *Notch1*^{fl/fl}; *Notch2*^{fl/fl} brains (Figure 2D) is not strictly adequate (*Notch* deletion by electroporation in a sparse population among normal cells versus the *Reeler* mutant), Figure 2F implies the similarity between the migration defect caused by Notch deficiency and that in *Reeler*. This abnormal positioning effect in *Notch1*^{fl/fl}; *Notch2*^{fl/fl} brains did not appear to be due to defects in neuronal/glial differentiation, progenitor proliferation rate, or the pattern of apoptotic cell death (Figures S6 and S7). Additionally, Reelin expression in the MZ also was not affected (Figure S7) and introduction of pTα1-IRES-Venus (without Cre) showed no effect in *Notch1*^{fl/fl}; *Notch2*^{fl/fl} brains (Figures 2E and 2F).

We next examined the distribution of the electroporated neurons at postnatal day 14 (P14), when neurons have settled into their final position. Most (over 90%) Venus^{+} neurons that electroporated with a Cre expression plasmid at E14.5 were located within layers II–IV in control (*Notch1*^{fl/+}; *Notch2*^{fl/+}) neocortex (Figures 3A and 3B). In contrast, in *Notch1*^{fl/fl}; *Notch2*^{fl/fl} cortex, fewer than half of Venus^{+} neurons were located within these layers, and instead over 50% of Venus+ neurons were found beneath layer IV (Figures 3C, 3D, and 3E). BrdU labeling of Venus^{+} cells 24 hr after electroporation confirmed similar results (Figures 3A, 3A′, and 3C–3C″). Further, *Notch*-deleted neurons expressing Cutl1 (also known as Cux1), a marker for layers II–IV, were abnormally positioned in deep neocortical layers in *Notch1*^{fl/fl}; *Notch2*^{fl/fl} brains compared with those of controls (Figures 3B, 3B′, and 3D–3D″). While the percentage of BrdU[+] or Cutl1^{+} cells in Venus-expressing neurons was similar between heterozygote and homozygote brains (BrdU: heterozygote, 27.45% ± 0.78%; homozygote, 26.15% ± 0.51%; p = not significant [n.s.] by Student's t test; Cutl1: heterozygote, 41.92% ± 1.06; homozygote, 39.66% ± 0.43; p = n.s. by Student's t test; the data represent the mean ± SEM of five brains each), Venus expression was undetectable in some displaced BrdU[+] or Cutl1^{+} neurons, suggesting that arrested neurons might cause the arrest of adjacent/nearby migrating neurons. These results demonstrate that Notch is required for neuronal migration in the neocortex, and the migration defect produced by the loss of Notch signaling results in a laminar displacement of neurons postnatally.

Notch Signaling Is Required for Proper Morphology of Migrating Neurons

The abnormal morphology of Reelin-signal-deficient neurons has been documented and is suspected to contribute to the disrup-
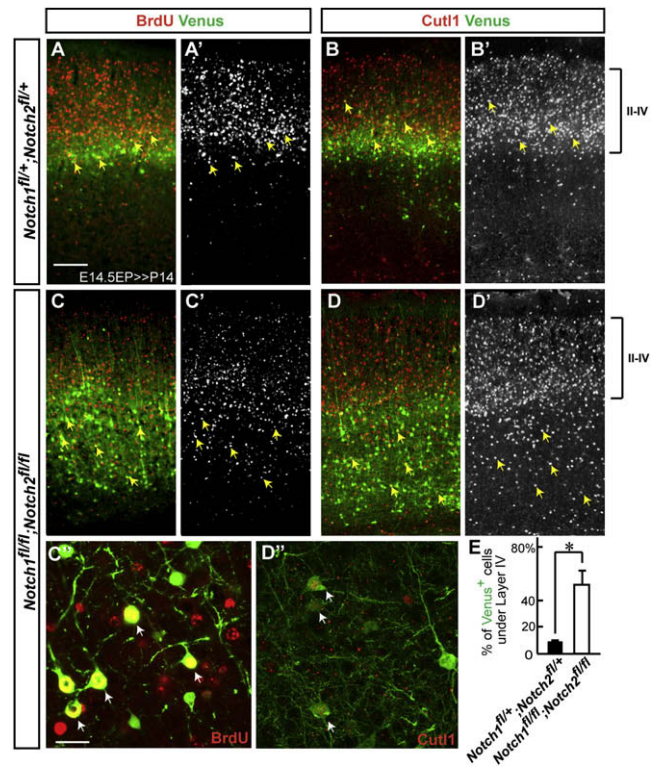

Figure 3. *Notch* Deletion Causes Laminar Displacement of Later-Born Neurons

(A–D″) Venus (green) immunostaining with BrdU or Cutl1 (red or white) staining in indicated mutants at P14. Note that Cutl1 analysis was performed in the dorsal somatosensory region where endogenous Cutl1 expression in lower layers is normally absent. BrdU[+]/Venus[+] or Cutl1^{+}/Venus^{+} neurons in the *Notch*-deleted cortex (C–D′, arrows) are abnormally positioned in lower layers when compared with the control cortex ([A–B′], arrows). (C″ and D″) Higher-magnification views of BrdU[+]/Venus[+] and Cutl1^{+}/Venus[+] double-labeled neurons around layer V, respectively (arrows). Bars = 100 μm (A–D′); 10 μm (C″ and D″). (E) Quantification of the distribution of Venus^{+} neurons under layer IV in the *Notch1*^{fl/+}; *Notch2*^{fl/+} and *Notch1*^{fl/fl}; *Notch2*^{fl/fl} cortex. The data represent the mean ± SEM of four brains each from independent experiments. *p < 0.005, Student's t test.

ted positioning of these neurons (Pinto-Lord et al., 1982; Sanada et al., 2004; Olson et al., 2006). We next examined whether Notch signal-deficient migrating neurons exhibit similar morphological defects to those observed in *Reeler*. Venus-labeled neurons in wild-type extended a long process toward the MZ (Figures 4A and 4A′); however, as previously described, neurons in *Reeler* retained stunted, bifarious, or multifarious leading processes (Figures 4B and 4B′). Similarly, *Notch*-targeted neurons exhibited shorter, multiple, and inconsistently oriented processes protruding directly from the cell soma (Figures 4C–4F). Thus, Reelin and Notch signaling-deficient migrating neurons share similar migratory and morphological abnormalities.

Forced Expression of Notch ICD Mitigates the Migration Defect Caused by Reelin Signal Deficiency

The above results showed phenotypic similarities between *Reelin*- and *Notch*-deleted neurons as well as reduction of Notch
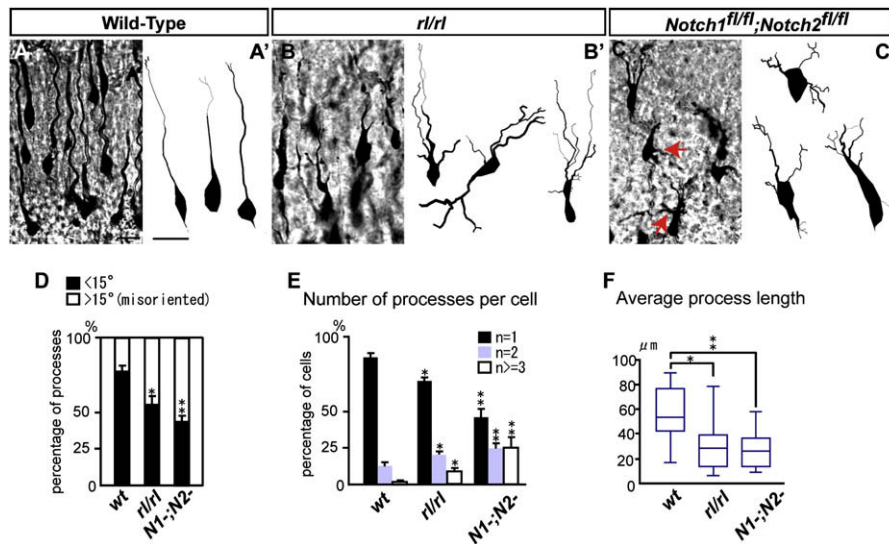
Figure 4. Morphological Defects in Migrating Neurons after Loss of Notch Signaling

(A–C) Venus immunostaining with pTα1-Cre-IRES-Venus revealed migrating neuronal morphology 3 days postelectroporation in wild-type, *Reeler*, and *Notch1 fl/fl; Notch2 fl/fl* mice. Red arrows in (C) indicate ectopic primary processes. (A′–C′) 3D reconstruction of Venus+ migrating neurons in mice of each genotype 3 days postelectroporation.

(D) Percentage of primary processes (directly protruded from cells) oriented normally (defined according to their angle toward the pial surface within ± 15°) and abnormally. *p < 0.01, **p < 0.001, Student's t test comparing with WT.

(E) Percentage of cells with one (black), two (blue), or more than three (white) processes per cell. *p < 0.05, **p < 0.01, Student's t test comparing corresponding bins to WT.

(F) Box plots of the average primary process length per cell (total process length/number of the primary processes). *p < 0.05, **p < 0.01, Mann-Whitney's U test. A total of 120 cells/genotype from four brains (different litters) were analyzed for orientation (D) and number of processes (E). The box plots of primary process length (F) were obtained for each genotype (n = 30 each from three brains [different litters]). Bars = 10 μm.

ICD in *Reeler* brains, but a functional interaction between these signaling pathways remains to be examined. Thus, to examine a potential interaction between Reelin and Notch signaling, we tested whether forced expression of Notch ICD in migrating neurons can affect the *Reeler* phenotype. Here we used the method from gene deletion experiments, in which postmitotic-neuron-enriched Cre/loxP recombination was confirmed (Figures 2, 3, S3, and S4). Thus, we electroporated pTα1-Cre-IRES-Venus into wild-type mice, *Reeler* mice, and mice with a compound background of *Reeler* and *Loxp-Stop-Loxp-Notch ICD* (rl/rl;LSL-Notch ICD), in which Notch ICD expression can be induced after Cre/loxP recombination. In wild-type mice 4 days postelectroporation, Venus+ neurons migrated into the upper layers in the CP (Figure 5A). As expected, Venus+ neurons were arrested in deeper layers in *Reeler* (Figure 5B). Strikingly, in rl/rl;LSL-Notch ICD mice, significantly fewer electroporated neurons were arrested in deeper cortical layers as compared with those of *Reeler* (Figures 5B, 5C, and 5E). Instead, a significant number of Venus+ neurons in which Notch ICD was replenished in the *Reeler* background migrated into the upper layers (Figure 5C). The transcription factor Tbr1, which is strongly expressed in deeper layers (primarily subplate and layer VI) and Cajal-Retzius cells in wild-type, is abnormally located in the upper layers in *Reeler* neocortex (Hevner et al., 2003). Venus+ electroporated neurons in *Reeler* cortex migrated past these Tbr1+ neurons (Figure 5C′), and some were found within the most superficial superplate (SPP). Farther migration of Notch-ICD-replenished neurons as compared to that of Reelin-signal-deficient neurons can be observed as early as 3.5 days postelectroporation, suggesting that replenishment of Notch ICD might mitigate the slower migration of Reelin-signal-deficient neurons (Sanada et al., 2004; Figure S8). These neurons remained in the upper layers even in the postnatal cortex (P3) (Figures 5F–5G″). BrdU injection at E15.5 revealed that BrdU+ neurons outside the electroporated region were distributed in lower layers of the *Reeler* CP, while the Venus+/BrdU+ electroporated neurons reached upper layers (Figures 5F and 5F′).

One characteristic of Reelin-signaling-deficient neurons is that terminally positioned neurons exhibit abnormally oriented dendrites (Pinto-Lord et al., 1982; Pinto-Lord and Caviness, 1979). Similarly, we found that, at 4.5 days postelectroporation (E19) and at P3, more mature, Notch-ICD-introduced neurons in the SPP also displayed abnormally orientated dendrites (arrowheads in Figure 5D, and data not shown). In contrast, overexpression of Notch ICD mitigated the morphological defects typical of migrating Reelin-signal-deficient neurons, and reduced the number of multifarious leading process (at 3 days after electroporation; Figures 6A–6D). Further, many of these electroporated migrating neurons exhibited a long process that oriented toward the MZ (compare Figures 6A and 6A′ with Figure 4B and 4B′). We did not observe obvious phenotypes in neuronal distribution, neurogenesis, and radial glial morphology by overexpression of Notch ICD in *LSL-Notch ICD* (Figure S9 and S10). Thus, these results indicate that in *Reeler* background, Notch ICD plays a significant
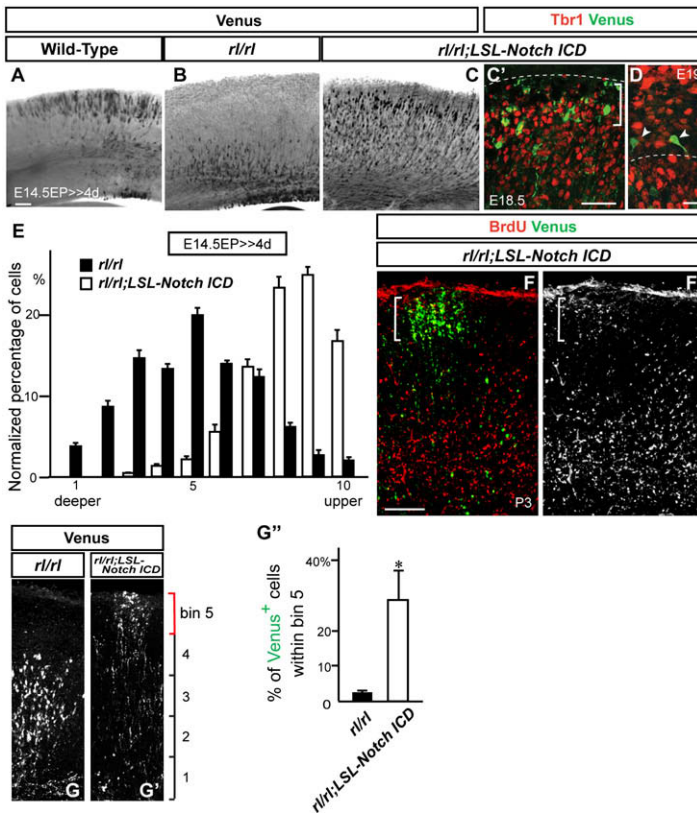
Figure 5. Replenished Notch ICD Mitigates Neuronal Migration Defects in *Reeler*

(A–D) Immunostaining for Venus (black, green) and Tbr1 (red) in cortical slices of indicated genotypes 4 days (A–C′) or 4.5 days (D) postelectroporation (with pTα1-Cre-IRES-Venus). (D) Higher-magnification view around the SPP. Dashed lines in (C′) and (D) indicate the pial surface and the border between the SPP and CP, respectively. Bracket in (C′) shows the SPP region. Note that electroporated Venus⁺ cells did not change their fate to Tbr1⁺ early-born neurons (C′ and D).

(E) Quantification of neuronal distribution shows significantly more cells in upper CP of *rl/rl;LSL-Notch ICD* when compared with *rl/rl* cortex [K-S test, $p < 0.0001$; repeated-measures ANOVA, $F_{(9,54)} = 18.91$, $p < 0.0001$]. The data represent the mean ± SEM of six brains each.

(F and F′) Immunostaining for Venus (green) and BrdU (red, white) in P3 cortical slices of *rl/rl;LSL-Notch ICD* electroporated with pTα1-Cre-IRES-Venus. Note that Venus⁺/BrdU⁺ cells (indicated by bracket) located over BrdU⁺ cells in surrounding lower layers.

(G and G′) Venus immunostaining in P3 cortical slices of *rl/rl* and *rl/rl;LSL-Notch ICD* electroporated with pTα1-Cre-IRES-Venus. (G″) Quantification of Venus⁺ neurons located in the upper part of the CP (within bin 5, indicated by a red bracket in [G] and [G′]; entire thickness of the cortex was subdivided into five bins.) The data represent the mean ± SEM of three brains each. *$p < 0.05$, Student's t test. Bars = 100 μm (A–C′ and F–G′); 20 μm (D).

role in neuronal migration, but likely not in determination of final dendritic orientation.

Replenishing Notch Activity Mitigates Neuronal Migration Defects Induced by Disrupted Dab1 Signaling

To rule out the possibility that the above alleviation effects appear only in the *Reeler* background where all cells (in addition to the electroporated cells) lack exposure to Reelin, we next tested whether Notch replenishment can mitigate the migration defect cell-autonomously within a wild-type background. Since Dab1 is a critical mediator of Reelin signaling and *Dab1* null mice display a similar phenotype to *Reeler* (Sheldon et al., 1997; Howell et al., 1997; Ware et al., 1997), we electroporated a dominant-negative mutant of Dab1 (5YF, a Reelin-signal-insensitive mutant) (Howell et al., 2000; Keshvara et al., 2001) into *LSL-Notch ICD* cortex (no exogenous Notch ICD is introduced without Cre recombinase). 5YF was sufficient to induce a migration defect [Figures 7A and 7B, Kolmogorov-Smirnov (K-S) test between 5YF and vector only control yields $p < 0.001$; ANOVA, $F_{(9,36)} = 12.61$, $p < 0.0001$] and served as a cell-autonomous model of Reelin signal deficiency as reported previously (Sanada et al., 2004). We were able to mitigate the 5YF-mediated migration defect by simultaneous introduction of Notch ICD through Cre-mediated recombination (Figures 7C and 7D). Fewer neurons were located near the IZ (bins 2–5 in Figure 7D) while more neurons reached the upper CP when compared with 5YF alone (bins 7–10 in Figure 7D). The mitigating effect appeared to be Reelin pathway specific since Notch ICD

overexpression was unable to mitigate the displacement of neurons lacking MEK kinase 4 (MEKK4; Sarkisian et al., 2006), a signaling pathway considered independent of Reelin (Figure S11). The mitigating effect by Notch signaling activity was further examined in P14 brains by another approach: electroporation was performed at E14.5 with pTα1-Cre-IRES-Venus, 5YF, and either CALSL-Notch ICD or CALSL-caRbpj (the constitutively active form of Rbpj). Through Cre-mediated recombination, expression of Notch ICD or caRbpj was driven from the CALSL plasmid (Matsuda and Cepko, 2007) in migrating neurons (data not shown), and we confirmed that both Notch ICD and caRbpj can mitigate the positioning defect of neurons caused by 5YF (Figures 7E–7H). Together, these results demonstrate that Notch ICD and Rbpj are involved in Reelin-Dab1 signaling-mediated control of neuronal migration.

Reelin-Stimulated Dab1 Blocks Degradation of Notch ICD

Based on the findings that nuclear Notch1 ICD is reduced in *Reeler* and that Dab1 binds Notch1 ICD (Figure 1), we investigated possible molecular mechanisms by which the Reelin-Dab1 pathway regulates levels of nuclear Notch ICD. Notch ICD is known to be degraded by a proteasome pathway via various E3 ubiquitin ligases (Lai, 2002), and Dab1 has been shown to inhibit the function of these ligases (Park et al., 2003). Furthermore, Dab1 is an adaptor protein that can control subcellular protein trafficking (Stolt and Bock, 2006; Honda and Nakajima, 2006; Hoe et al., 2006), which is a critical step in protein
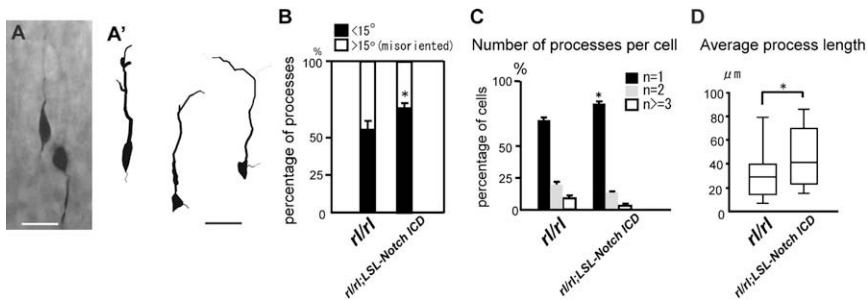
Figure 6. Replenished Notch ICD Mitigates Morphological Defects in *Reeler*

(A) Venus+ neurons 3 days postelectroporation with pTα1-Cre-IRES-Venus in *rl/rl;LSL-Notch ICD* mice. Left neuron in (A) shows rescued morphology with processes that are more pial-oriented compared with *rl/rl* (e.g., Figure 4B). (A') 3D reconstruction of Venus+ neurons (compare with *rl/rl* in Figure 4B').

(B–D) Quantification of direction of primary processes (B), primary process number per cell (C), and average primary process length per cell (D) for the electroporated neurons in mice of indicated genotypes. *p < 0.05, Student's t test (B and C), *p < 0.05, Mann-Whitney's U test (D). A total of 120 cells/genotype from four independent experiments were analyzed for orientation (B) and number of processes (C). The box plots of primary process length (D) were obtained for each genotype (n = 30 each from three independent experimental sets). For better comparison with *Reeler*, duplicated data from Figure 4 were included. Bars = 10 μm.

degradation. Thus, we hypothesized that Reelin-Dab1 signaling may regulate this degradation pathway by stabilizing and/or controlling the levels of Notch ICD. To assess the influence of Reelin-Dab1 signaling on Notch activity via the proteasome pathway, we measured Rbpj luciferase reporter expression levels in Cos-7 cells. Reporter expression is induced by introduction of Notch ICD, the level of which can be controlled by introduction of Fbxw7 (also known as Sel-10 or Cdc4), an adaptor molecule of E3 ligase that leads to degradation of Notch ICD (Gupta-Rossi et al., 2001; Oberg et al., 2001; Wu et al., 2001). Consistent with previous reports, transfection with Notch ICD led to robust induction of luciferase expression (Figure 8A, compare lane 7 with 1), which was reduced by cointroduction of Fbxw7 (Figure 8A, lane 13). Cotransfection of wild-type Dab1 with the constitutively active form of Src kinase (caSrc), a condition that recapitulates Reelin-signal-stimulated Dab1 activation in vitro (Bock and Herz, 2003), significantly blocked the reduction of reporter activity due to Fbxw7 (Figure 8A, compare lane 16 with 13). In contrast, the 5YF mutant of Dab1 did not elicit enhanced reporter activity (Figure 8A, p = n.s. between lane 13 and 18). Dab1 did not affect the reporter activities when Fbxw7 was not transfected (Figure 8A, lane 1–12). These results suggest that Reelin-stimulated Dab1 might protect Notch ICD from Fbxw7-induced degradation. Additionally, Fbxw7-mediated reduction of Notch ICD levels and enhancement of its polyubiquitination in Cos-7 cells was significantly inhibited in the presence of wild-type, but not the 5YF mutant form of, Dab1 (Figure 8B, data not shown, n = 5). Thus, our in vitro experiments indicate that Reelin-Dab1 signaling can inhibit Notch ICD degradation through the Fbxw7-mediated pathway.

The experiments described above can precisely control the activities of both Reelin and Notch signaling, but the system is relatively artificial. Thus, to gain further evidence, we next examined whether the ubiquitination of Notch is actually affected by Reelin deficiency during cortical development. Slices were prepared from wild-type and *Reeler* brains. We then made lysates from noncultured slices or slices cultured for 4 hr in the presence of proteasome inhibitors to allow accumulation of the polyubiquitinated proteins by inhibiting their degradation, immunoprecipitated Notch1 ICD, and immunoblotted using an anti-polyubiquitin antibody. Consistent with results in Cos-7 cells, we observed a noticeable increase of polyubiquitin bands in *Reeler* both with and without protease inhibitors (Figure 8C, compare lanes 1

and 4 with lanes 2/3 and 5/6, respectively; n > 3 per each genotype). Since we were unable to determine whether Notch1 ICD was specifically polyubiquitinated in this system (because we could not obtain enough precipitate from brain lysates using either anti-Notch1 ICD [Val 1744] or anti-polyubiquitin antibodies), we confirmed specific ubiquitination of nuclear Notch1 ICD by using Notch1-ICD-transfected cortical neurons in vitro (Figure 8D, n = 3). Stimulation by Reelin-containing medium significantly reduced polyubiquitinated Notch1 ICD (compare lane 2 with 1) and this was inhibited by addition of Dab1 5YF (lane 6) but not wild-type Dab1 (lane 4). Altogether, these data suggest that Notch1 ICD is likely targeted by the Reelin signaling pathway during cortical development and suggest that Reelin-Dab1 signaling prevents Notch ICD degradation.

DISCUSSION

Despite over half a century of research since the first report of *Reeler*, the underlying pathogenetic mechanisms still remain unclear. Disruptions in several developmental processes have been proposed to cause the phenotype. First, the actin cytoskeleton of Reelin-signaling-deficient neurons is abnormally organized, which may lead to disruption of the leading process and subsequent failed migration (Pinto-Lord and Caviness, 1979; Sanada et al., 2004; Olson et al., 2006). Second, Reelin-deficient neurons may fail to detach from radial glia at the appropriate position as a result of increased neuron-glia adhesion due to abnormally high levels of α3 integrin (Sanada et al., 2004). Additionally, the aberrantly superficial positioning of early-generated neurons may physically obstruct the migration of later-born neurons, thereby giving rise to an inverted lamination of the cortex (Pinto-Lord and Caviness, 1979; Tabata and Nakajima, 2002).

To explore Notch's potential role in migration, we employed a methodology that could circumvent the complications introduced by traditional knockout and transgenic strategies, which are unable to discriminate among Notch deletion defects due to proliferation, differentiation, or apoptosis. Using this approach, we provide evidence that the morphology and migration of postmitotic neurons is regulated by Notch signaling, whose activity is likely under the control of the Reelin-Dab1 pathway. We observed that both the nuclear Notch ICD expression and Notch ICD activity-dependent Rbpj-mediated transcription typical of wild-type migrating neurons were significantly reduced in
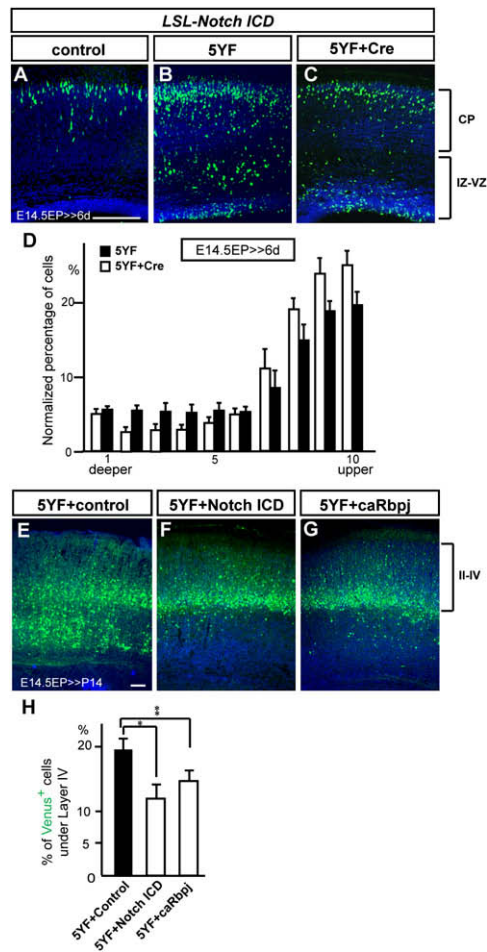
Figure 7. Notch ICD Mitigates Radial Migration Defects Induced by a Dominant-Negative Form of Dab1

(A–C) Venus^{+} neurons were detected by immunohistochemistry 6 days after electroporation with pCDNA3.1 empty (A) or containing Dab1 5YF (B and C) plasmid with pTα1-IRES-Venus (A and B) or pTα1-Cre-IRES-Venus (C) plasmid in *LSL-Notch ICD* mice. Note that 5YF arrested many neurons beneath the CP, a condition which was mitigated by overexpression of Notch ICD.

(D) Quantification of neuronal distribution in the *LSL-Notch ICD* cortex electroporated with indicated plasmids [K-S test, $p < 0.05$; repeated-measures ANOVA, $F(9,126) = 5.24$, $p < 0.05$]. The data represent the mean ± SEM of six brains each.

(E–G) Venus^{+} neurons were detected by immunohistochemistry at P14 after E14.5 electroporation with pCALSL empty (E), containing Notch ICD (F), or caRbpj (G) with pTα1-Cre-IRES-Venus and pCDNA3.1-Dab1 5YF plasmids in wild-type mice. Note that compared with control (E), overexpression of Notch ICD (F) or caRbpj (G) resulted in fewer neurons located beneath layer IV.

(H) Percentages of Venus^{+} neurons below layer IV in P14 wild-type cortex electroporated with indicated plasmids. The data represent the mean ± SEM of 10, 8, and 11 brains, respectively. *$p < 0.01$, **$p < 0.05$ by Student's t test. Bars = 100 μm.

Reeler cortex (Figure 1 and S3). These findings are consistent with a report that the expression of the Notch target gene, *Strawberry Notch,* is also downregulated in *Reeler* (Baba et al., 2006).

To explore the consequence of the observed reductions in active Notch ICD and downstream signaling, we deleted *Notch* in migrating neurons and observed morphological and migration defects similar to those of Reelin-signal-deficient neurons (Figures 2–4). Furthermore, introducing Notch ICD or caRbpj mitigated migration defects observed in Reelin-Dab1-signaling-deficient neurons in wild-type (or *LSL-Notch ICD*) background (Figure 7) as well as those in the *Reeler* background (Figures 5, 6, and S8). Thus, Notch signaling appears to play a cell-autonomous role during neuronal migration. Finally, replenished Notch ICD was able to alleviate migrating neuronal morphology, but was not sufficient to reorient the dendrites of matured neurons in *Reeler* (Figures 5 and 6). This suggests that Notch signaling is required during migration. but not during final maturation stages that include somal and dendritic orientation. Alternatively, disruption of the latter may be secondary to the abnormal formation of the internal plexiform zones in *Reeler* as previously suggested (Pinto-Lord and Caviness, 1979; Tabata and Nakajima, 2002). Consistent with this physical barrier hypothesis, we (this study, data not shown) and others (Sanada et al., 2004; Olson et al., 2006) did not observe neurons with inverted dendrites after cell-autonomous reduction of Reelin-Dab1 signaling by 5YF or Dab1 shRNA introduction. Whether the superficial positioning of early-born neurons in the *Reeler* cortex forms a physical barrier to migration is unclear; however, reintroduction of Notch ICD enabled later-born Reelin-signal-deficient neurons to migrate past the abnormally superficial band of early-born neurons (including subplate neurons) to reach the upper layers (Figure 5). Thus, it is possible that the positioning of later-born neurons in *Reeler* is due to a cell-autonomous migration defect rather than physical obstruction. Interestingly, similar alleviation effects can be achieved by expressing Reelin in *Reeler* VZ cells (Magdaleno et al., 2002), suggesting that migrating neurons may require Reelin stimulation and Notch activation much earlier than previously suspected (i.e., before they arrive in the CP). These results support the model that Reelin signaling works as "an instructive signal" (D'Arcangelo et al., 1997) to engage cytoskeletal remodeling events critical to neuronal migration.

Both Notch- and Reelin-signaling-deficient neurons exhibit processes with disrupted morphology (Figure 4). These morphological defects may be a result of premature terminal differentiation of dendrites. However, given that neuronal maturation correlates with an increase of Notch ICD (our Figure 1; Šestan et al., 1999), premature terminal differentiation by Notch reduction/deletion is unlikely. Alternatively, the transition from the multipolar to bipolar stage—a critical step during proper neuronal migration (LoTurco and Bai, 2006)—might be impaired. While common transitional defects occur mostly within the SVZ to IZ and our *Notch*-targeted defects were observed mainly in the lower CP, these differences may simply reflect our methodological approach for gene knockdown (e.g., Tα1-promoter-driven Cre/loxP system versus U6-promoter-driven shRNA). Nevertheless, given that Reelin can regulate actin dynamics in neurons (e.g., Suetsugu et al., 2004; Chen et al., 2004), the morphological defects seen in Reelin- or Notch-deficient migrating neurons most likely reflect specific disruptions of the leading process. A recent study has shown that Notch ligands are specifically displayed by intermediate progenitors in the SVZ and young neurons in the IZ during the period of neurogenesis and neuronal migration (Yoon et al., 2008). Given the significant migration arrest of Notch-deficient neurons in the IZ to lower CP (Figure 2),
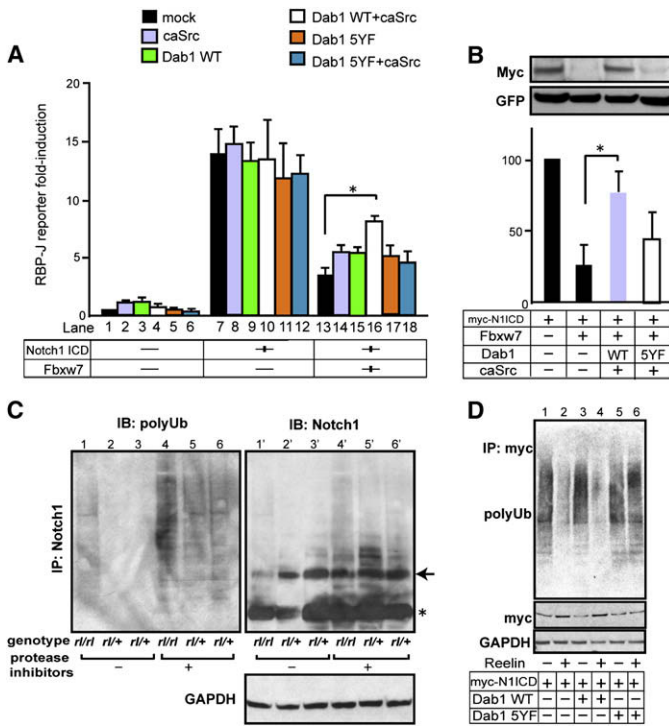
Figure 8. Stimulated Dab1 Blocks Notch ICD Degradation

(A) Effects of active Dab1 on Notch ICD activity. Relative Rbpj luciferase activity of each condition is compared to lane 1 set as 1.0. The indicated values are the mean ± SEM of three experiments performed in triplicate. *p < 0.05, Student's t test.

(B) Cos-7 cells were transfected with indicated plasmids, and the expression of Notch1 ICD and GFP (as an internal control, reprobed on the same membrane) were analyzed by IB. The graphs show the relative intensity of the Notch1 ICD against the left lane after normalization with GFP as a transfection control. The data represent the mean ± SEM of three independent experiments. *p < 0.01, paired t test. Transfection of caSrc without Dab1 or Dab1 without caSrc constructs gave equivalent results to Dab1 5YF with/without caSrc. Transfection of caSrc with/without Dab1 constructs did not alter either endogenous or exogenous Fbxw7 expression levels (data not shown).

(C) IB of lysates from rl/rl and rl/+ brain slices against polyubiquitin (FK2) and Notch1 after IP with a Notch1 antibody. IB against GAPDH was obtained from the flowthrough of IP. The samples in the left three lanes were obtained from freshly prepared cortical slices, and the samples in right three lanes were from slices cultured with proteasome inhibitors. Note the decrease of precipitated nonpolyubiquitinated Notch1 in *Reeler* (lanes 1′ and 4′), consistent with the increase of polyubiquitinated Notch1 (lanes 1 and 4). Arrow indicates p100-p120 Notch1 ICD bands. Asterisk shows IgG bands.

(D) IB of lysates from cultured cortical neurons transfected with the indicated plasmids against polyubiquitin (FK2) and myc after IP with a myc antibody. The transfected neurons were exposed to Reelin containing- or mock medium for 6 hr with protease inhibitors before collection. IB against GAPDH was obtained from the IP flowthrough.

an intriguing possibility is that Notch ligands displayed in the IZ are critical for radial movement of neurons.

Our finding of a dose-dependent Notch deletion effect on radial neuronal migration (with *Notch1 fl/fl; Notch2 fl/+* < *Notch1 fl/fl; Notch2 fl/fl* as the most severe defect; see Figure S5) supports our model that reduced Notch activity, rather than a complete loss of its activity, can lead to migration defects in *Reeler*. In agreement with previous reports (Yoon and Gaiano, 2005; Louvi and Artavanis-Tsakonas, 2006), this finding also supports the pleiotropy of Notch signaling in an activity-level-dependent manner. Therefore Notch processing and activity is precisely controlled at various stages (Bray, 2006), and we now implicate Reelin signaling in this regulation. Our results suggest that Reelin signaling may govern the level of nuclear Notch ICD levels by affecting Notch ICD degradation. We show that Notch polyubiquitination/degradation is increased in *Reeler* cortex, and that degradation of Notch ICD through the Fbxw7-mediated proteasome pathway is inhibited by activated Dab1 in vitro (Figure 8). However, Reelin signaling also promotes Dab1 degradation (Arnaud et al., 2003; Bock et al., 2004; Kuo et al., 2005; Feng et al., 2007), which at first glance does not fit to our model. Interestingly, studies have shown that Dab1 could function in the trafficking of some molecules (Honda and Nakajima, 2006; Hoe et al., 2006), suggesting that Dab1 could potentially serve to traffic Notch ICD, thereby sequestering it away from the degradation pathway. It is also noteworthy that alteration of Notch intracellular distribution (trafficking) can significantly affect its degradation rate and activity (Mukherjee et al., 2005). Fbxw7-mediated Notch ICD ubiquitination can occur specifically within the nucleus (Gupta-Rossi et al., 2001). We did not determine whether Fbxw7 mediates Notch degradation during neuronal migration, but we did observe specific expression of Fbxw7 in

migrating neurons (K.H.-T. and P.R., unpublished data). Therefore, Reelin-Dab1 signaling may facilitate the trafficking of Notch ICD to reduce its degradation via Fbxw7 in the developing neocortex.

Additional mechanisms could also control the ubiquitin-mediated degradation of Notch ICD. For example, a complex of Numb and Itch E3 ubiquitin ligase mediates lysosomal degradation of Notch ICD in the cytoplasm (McGill and McGlade, 2003). Both Numb and Dab1 contain a PTB domain that exhibits similar binding and functional properties (Lai, 2002). Thus, Dab1 and Numb may compete for Notch binding and thereby regulate degradation. Alternatively, inhibition of Notch ICD degradation may be achieved by direct binding of Dab1 to E3 ubiquitin ligases to block its ubiquitination activity (Park et al., 2003), or simple competition for the same E3 ligases for its degradation with Notch ICD. Although Notch cleavage processing was not significantly affected in *Reeler* (Figure 1), we did not formally examine the possible effects of Reelin signaling on Notch processing. Therefore a weaker interaction between Notch and Reelin signaling may exist at this level, similar to the mechanism whereby Reelin-Dab1 signaling promotes APP processing and trafficking (Hoe et al., 2006).

Although our study showed an interaction of Notch and Reelin signaling pathways in the control of radial migration of cortical neurons, it remains to be examined whether the defect of this interaction underlies *Reeler* phenotypes besides impaired neuronal migration, such as radial glial dysmorphology (Dulabon et al., 2000; Forster et al., 2002; Hartfuss et al., 2003) and neuronal invasion into layer I (Trommsdorff et al., 1999; Hack et al., 2007). Considering that Notch and Reelin signaling directly control the expression of BLBP, a radial glial gene (Hartfuss et al., 2003; Anthony et al., 2005), radial glial development might be

regulated by the interaction between Reelin and Notch signaling. During the review period of this paper, a study reported that a Dab1-Notch ICD interaction and a Reelin-dependent increase of Notch1 are reproducible in a human neural progenitor cell line (Keilani and Sugaya, 2008), supporting this possibility. Future studies will test these possibilities using total brain-specific deletion of *Notch* and determine whether it reproduces *Reeler* phenotypes in other various aspects of brain development.

EXPERIMENTAL PROCEDURES

Mice
Reeler and *Scrambler* mice were purchased from Jackson Laboratory. The tissues and lysates of *Vldlr/ApoER2* dKO mice were generous gifts from Drs. A. Goffinet and Y. Jossin. Generation and genotyping of *floxed Notch1*, *floxed Notch2*, *LSL-Notch ICD* (also known as *CALSL-NICD(H)*), and *LSL-Gfp* (transgene includes loxP-flanked STOP cassette followed by *Gfp*; Jackson Laboratory) mouse lines were described previously. A list of references for *floxed* mice is available as Supplemental Data. Animals were handled according to protocols approved by the Institutional Animal Care and Use Committee of Yale University School of Medicine.

Quantitative RT-PCR
Total RNA was isolated from freshly dissected brain tissue by using the Rneasy plus kit (QIAGEN), and cDNA was synthesized by using SuperScript First-strand synthesis system for RT-PCR with random hexamer primers (Invitrogen). *GAPDH* levels were detected by Taqman rodent GAPDH control reagents and used for normalization. Thermocycling was carried out by using the Applied Biosystems 7900 system and monitored by SYBR Green I dye detection. All reactions were performed in triplicate from four brains each.

In Utero Electroporation
In utero electroporation was performed at E14.5 as previously described (Sarkisian et al., 2006). A list of DNA solutions used for injection is available as Supplemental Data. All control experiments were performed using empty vectors at the same concentrations. All BrdU labeling was performed 24 hr after electroporation according to previous studies (Sarkisian et al., 2006).

Immunohistochemistry and Data Analysis
Immunohistochemistry was performed with the previously described methods (Sarkisian et al., 2006). A list of antibodies is available as Supplemental Data. Electroporated neurons around the somatosensory medial cortical region were counted for all positioning analyses. Tracing of the morphology, and quantification of orientation, number of processes, and length of the processes protruded from Venus^{+} neurons were done by the Neurolucida system (MicroBrightfield). In these analyses, we chose neurons located in the lower CP close to the IZ, and excluded terminal branches of processes in the MZ for quantification. Axons were excluded from both tracing and quantification. In box plot analysis, the line in the box and the upper and lower edge of the box indicate the median and the 25th and 75th percentiles, respectively. Error bars indicate the 5th and 95th percentiles.

Immunoprecipitation and Immunoblotting
Protein samples from E18.5 or P0 mouse brain were harvested and used for immunoprecipitation and immunoblotting using a standard protocol. The antibodies used for immunoprecipitations and immunoblots are listed in Supplemental Data. Analysis of band intensity was performed as previously described (Sarkisian et al., 2006).

Luciferase Assay
Subconfluent Cos-7 cells were transiently transfected with plasmids at 50 ng (caSrc), 200 ng (pGL2-8xCBF-luc and phRL), or 500 ng (myc-Notch ICD, Fbxw7, and Dab1 constructs) per well into 12-well plates. An equal amount of control construct (pCDNA3.1 empty vector) was transfected in mock experiments. The cells were subjected to the assay using Dual-Luciferase Reporter Assay system (Promega) 1 day after transfection. For the detection of luciferase activity, TD-20/20 (Turner Designs) was used.

Ubiquitination Assay
By using Fugene6 (Roche), subconfluent Cos-7 cells were transiently transfected with the plasmids containing Dab1, Notch1 ICD, Fbxw7 and pCDNA3.1-HA-Ub, and pCAG-GFP, and harvested 48 hr later. Proteasome inhibitors MG-132 and clasto-lactacystin β-Lactone (Calbiochem) were added at 10 μM 6 hr before harvest. For slice culture of E18.5 cerebral cortex, chopped slices at 300 μm thickness were incubated on the membrane floating in the Neurobasal medium with proteasome inhibitors for 4 hr. Cortical neurons were prepared for primary culture from dissected E18.5 cortex, and transfected with the plasmids using amaxa Nucleofector Kit (Lonza). Reelin containing- or mock medium was prepared from 293T cells transfected with pCrl or pCDNA-EGFP, respectively, as described (Honda and Nakajima, 2006), and applied with the proteasome inhibitors to the culture 2 days after passage.

Additional information related to DNA constructs is included in the Supplemental Data.

SUPPLEMENTAL DATA

The supplemental data for this article contain 11 Figures, Supplemental Text, and Supplemental Experimental Procedures and can be found at http://www.neuron.org/supplemental/S0896-6273(08)00800-3.

REFERENCES

Anthony, T.E., Mason, H.A., Gridley, T., Fishell, G., and Heintz, N. (2005). Brain lipid-binding protein is a direct target of Notch signaling in radial glial cells. Genes Dev. *19*, 1028–1033.

Arnaud, L., Balif, B.A., and Cooper, J.A. (2003). Regulation of protein tyrosine kinase signaling by substrate degradation during brain development. Mol. Cell. Biol. *23*, 9293–9302.

Ayala, R., Shu, T., and Tsai, L.H. (2007). Trekking across the brain: the journey of neuronal migration. Cell *128*, 29–43.

Baba, K., Dekimoto, H., Muraoka, D., Agata, K., Terashima, T., and Katsuyama, Y. (2006). A mouse homologue of Strawberry Notch is transcriptionally regulated by Reelin signal. Biochem. Biophys. Res. Commun. *350*, 842–849.

Ballif, B.A., Arnaud, L., Arthur, W.T., Guris, D., Imamoto, A., and Cooper, J.A. (2004). Activation of a Dab1/CrkL/C3G/Rap1 pathway in Reelin-stimulated neurons. Curr. Biol. *14*, 606–610.

Bar, I., Lambert de Rouvroit, C., and Goffinet, A.M. (2000). The Reelin signaling pathway in mouse cortical development. Eur. J. Morphol. *38*, 321–325.

Bielas, S.L., and Gleeson, J.G. (2004). Cytoskeletal-associated proteins in the migration of cortical neurons. J. Neurobiol. *58*, 149–159.

Bock, H.H., Jossin, Y., Liu, P., Forster, E., May, P., Goffinet, A.M., and Herz, J. (2003). Phosphatidylinositol 3-Kinase Interacts with the adaptor protein Dab1 in Response to Reelin signaling and is Required for normal cortical lamination. J. Biol Chem. *278*, 38772–38779.

Bock, H.H., and Herz, J. (2003). Reelin activates SRC family tyrosine kinase in neurons. Curr. Biol. *13*, 18–26.

Bock, H.H., Jossin, Y., May, P., Bergner, O., and Herz, J. (2004). Apolipoprotein E receptors are required for reelin-induced proteasomal degradation of the neuronal adaptor protein Disabled-1. J. Biol. Chem. 279, 33471–33479.

Bray, S.J. (2006). Notch signalling: a simple pathway becomes complex. Nat. Rev. Mol. Cell Biol. 7, 678–689.

Caviness, V.S., Jr., and Rakic, P. (1978). Mechanisms of cortical development: a view from mutations in mice. Annu. Rev. Neurosci. 1, 297–326.

Chen, K., Ochalski, P.G., Tran, T.S., Sahir, N., Schubert, M., Pramatarova, A., and Howell, B.W. (2004). Interaction between Dab1 and CrkII is promoted by Reelin signaling. J. Cell Sci. 117, 4527–4536.

Coksaygan, T., Magnus, T., Cai, J., Mughal, M., Lepore, A., Xue, H., Fischer, I., and Rao, M.S. (2006). Neurogenesis in Talpha-1 tubulin transgenic mice during development and after injury. Exp. Neurol. 197, 475–485.

D'Arcangelo, G. (2006). Reelin mouse mutants as models of cortical development disorders. Epilepsy Behav. 8, 81–90.

D'Arcangelo, G., Nakajima, K., Miyata, T., Ogawa, M., Mikoshiba, K., and Curran, T. (1997). Reelin is a secreted glycoprotein recognized by the CR-50 monoclonal antibody. J. Neurosci. 17, 23–31.

D'Arcangelo, G., Homayouni, R., Keshvara, L., Rice, D.S., Sheldon, M., and Curran, T. (1999). Reelin is a ligand for lipoprotein receptors. Neuron 24, 471–479.

Dulabon, L., Olson, E.C., Taglienti, M.G., Eisenhuth, S., McGrath, B., Walsh, C.A., Kreidberg, J.A., and Anton, E.S. (2000). Reelin binds alpha3beta1 integrin and inhibits neuronal migration. Neuron 27, 33–44.

Feng, L., Allen, N.S., Simo, S., and Cooper, J.A. (2007). Cullin 5 regulates Dab1 protein levels and neuron positioning during cortical development. Genes Dev. 21, 2717–2730.

Forster, E., Tielsch, A., Saum, B., Weiss, K.H., Johanssen, C., Graus-Porta, D., Muller, U., and Frotscher, M. (2002). Reelin, Disabled 1, and beta 1 integrins are required for the formation of the radial glial scaffold in the hippocampus. Proc. Natl. Acad. Sci. USA 99, 13178–13183.

Forster, E., Jossin, Y., Zhao, S., Chai, X., Frotscher, M., and Goffinet, A.M. (2006). Recent progress in understanding the role of Reelin in radial neuronal migration, with specific emphasis on the dentate gyrus. Eur. J. Neurosci. 23, 901–909.

Gal, J.S., Morozov, Y.M., Ayoub, A.E., Chatterjee, M., Rakic, P., and Haydar, T.F. (2006). Molecular and morphological heterogeneity of neural precursors in the mouse neocortical proliferative zones. J. Neurosci. 26, 1045–1056.

Giniger, E. (1998). A role for Abl in Notch signaling. Neuron 20, 667–681.

Gloster, A., Wu, W., Speelman, A., Weiss, S., Causing, C., Pozniak, C., Reynolds, B., Chang, E., Toma, J.G., and Miller, F.D. (1994). The T alpha 1 alpha-tubulin promoter specifies gene expression as a function of neuronal growth and regeneration in transgenic mice. J. Neurosci. 14, 7319–7330.

Gupta-Rossi, N., Le Bail, O., Gonen, H., Brou, C., Logeat, F., Six, E., Ciechanover, A., and Israël, A. (2001). Functional interaction between SEL-10, an F-box protein, and the nuclear form of activated Notch1 receptor. J. Biol. Chem. 276, 34371–34378.

Hack, I., Hellwig, S., Jughans, D., Brunne, B., Bock, H.H., Zhao, S., and Frotscher, M. (2007). Divergent roles of ApoER2 and Vldlr in the migration of cortical neurons. Development 34, 3883–3891.

Hartfuss, E., Forster, E., Bock, H.H., Hack, M.A., Leprince, P., Luque, J.M., Herz, J., Frotscher, M., and Gotz, M. (2003). Reelin signaling directly affects radial glia morphology and biochemical maturation. Development 130, 4597–4609.

Hevner, R.F., Daza, R.A., Rubenstein, J.L., Stunnenberg, H., Olavarria, J.F., and Englund, C. (2003). Beyond laminar fate: toward a molecular classification of cortical projection/pyramidal neurons. Dev. Neurosci. 25, 139–151.

Hiesberger, T., Trommsdorff, M., Howell, B.W., Goffinet, A., Mumby, M.C., Cooper, J.A., and Herz, J. (1999). Direct binding of Reelin to VLDL receptor and ApoE receptor 2 induces tyrosine phosphorylation of disabled-1 and modulates tau phosphorylation. Neuron 24, 481–489.

Hoe, H.S., Tran, T.S., Matsuoka, Y., Howell, B.W., and Rebeck, G.W. (2006). DAB1 and Reelin effects on amyloid precursor protein and ApoE receptor 2 trafficking and processing. J. Biol. Chem. 281, 35176–35185.

Honda, T., and Nakajima, K. (2006). Mouse Disabled1 (DAB1) is a nucleocytoplasmic shuttling protein. J. Biol. Chem. 281, 38951–38965.

Hong, S.E., Shugart, Y.Y., Huang, D.T., Shahwan, S.A., Grant, P.E., Hourthane, J.O., Martin, N.D., and Walsh, C.A. (2000). Autosomal recessive lissencephaly with cerebellar hypoplasia is associated with human RELN mutations. Nat. Genet. 26, 93–96.

Howell, B.W., Hawkes, R., Soriano, P., and Cooper, J.A. (1997). Neuronal position in the developing brain is regulated by mouse disabled-1. Nature 389, 733–737.

Howell, B.W., Lanier, L.M., Frank, R., Gertler, F.B., and Cooper, J.A. (1999). The disabled 1 phosphotyrosine-binding domain binds to the internalization signals of transmembrane glycoproteins and to phospholipids. Mol. Cell. Biol. 19, 5179–5188.

Howell, B.W., Herrick, T.M., Hildebrand, J.D., Zhang, Y., and Cooper, J.A. (2000). Dab1 tyrosine phosphorylation sites relay positional signals during mouse brain development. Curr. Biol. 10, 877–885.

Jossin, Y., and Goffinet, A.M. (2007). Reelin signals through Phosphatidylinositol 3-Kinase and Akt to control cortical development and through mTor to regulate dendritic growth. Mol. Cell. Biol. 27, 7113–7124.

Kanatani, S., Tabata, H., and Nakajima, K. (2005). Neuronal migration in cortical development. J. Child Neurol. 20, 274–279.

Kawauchi, T., and Hoshino, M. (2008). Molecular pathways regulating cytoskeletal organization and morphological changes in migrating neurons. Dev. Neurosci. 30, 36–46.

Keilani, S., and Sugaya, K. (2008). Reelin induces a radial glial phenotype in human neural progenitor cells by activation of Notch-1. BMC Dev. Biol. 8, 69.

Keshvara, L., Benhayon, D., Magdaleno, S., and Curran, T. (2001). Identification of reelin-induced sites of tyrosyl phosphorylation on disabled 1. J. Biol. Chem. 276, 16008–16014.

Kohyama, J., Tokunaga, A., Fujita, Y., Miyoshi, H., Nagai, T., Miyawaki, A., Nakao, K., Matsuzaki, Y., and Okano, H. (2005). Visualization of spatiotemporal activation of Notch signaling: live monitoring and significance in neural development. Dev. Biol. 286, 311–325.

Kriegstein, A.R., and Noctor, S.C. (2004). Patterns of neuronal migration in the embryonic cortex. Trends Neurosci. 27, 392–399.

Kuo, G., Arnaud, L., Kronstad-O'Brien, P., and Cooper, J.A. (2005). Absence of Fyn and Src causes a reeler-like phenotype. J. Neurosci. 25, 8578–8586.

Lai, E.C. (2002). Protein degradation: four E3s for the notch pathway. Curr. Biol. 12, R74–R78.

Lambert de Rouvroit, C., and Goffinet, A.M. (2001). Neuronal migration. Mech. Dev. 105, 47–56.

Le Gall, M., and Giniger, E. (2004). Identification of two binding regions for the suppressor of hairless protein within the intracellular domain of Drosophila notch. J. Biol. Chem. 279, 29418–29426.

Le Gall, M., De Mattei, C., and Giniger, E. (2008). Molecular separation of two signaling pathways for the receptor, Notch. Dev. Biol. 313, 556–567.

LoTurco, J.J., and Bai, J. (2006). The multipolar stage and disruptions in neuronal migration. Trends Neurosci. 29, 407–413.

Louvi, A., and Artavanis-Tsakonas, S. (2006). Notch signalling in vertebrate neural development. Nat. Rev. Neurosci. 7, 93–102.

Magdaleno, S., and Curran, T. (2001). Brain Development: integrins and the Reelin pathway. Curr. Biol. 11, R1032–R1035.

Magdaleno, S., Keshvara, L., and Curran, T. (2002). Rescue of ataxia and preplate splitting by ectopic expression of Reelin in reeler mice. Neuron 33, 573–586.

Matsuda, T., and Cepko, C.L. (2007). Controlled expression of transgenes introduced by in vivo electroporation. Proc. Natl. Acad. Sci. USA 16, 1027–1032.

McGill, M.A., and McGlade, C.J. (2003). Mammalian numb proteins promote Notch1 receptor ubiquitination and degradation of the Notch1 intracellular domain. J. Biol. Chem. *278*, 23196–23203.

Mukherjee, A., Veraksa, A., Bauer, A., Rosse, C., Camonis, J., and Artavanis-Tsakonas, S. (2005). Regulation of Notch signaling by non-visual beta-arrestin. Nat. Cell Biol. *7*, 1159–1161.

Oberg, C., Pauley, A., Wolf, E., Gurney, M., and Lendahl, U. (2001). The Notch intracellular domain is ubiquitinated and negatively regulated by the mammalian Sel-10 homolog. J. Biol. Chem. *276*, 35847–35853.

Ohtsuka, T., Imayoshi, I., Shimojo, H., Nishi, E., Kageyama, R., and McConnell, S.K. (2006). Visualization of embryonic neural stem cells using Hes promoters in transgenic mice. Mol. Cell. Neurosci. *31*, 109–122.

Olson, E.C., and Walsh, C.A. (2002). Smooth, rough and upside-down neocortical development. Curr. Opin. Genet. Dev. *12*, 320–327.

Olson, E.C., Kim, S., and Walsh, C.A. (2006). Impaired neuronal positioning and dendritogenesis in the neocortex after cell-autonomous Dab1 suppression. J. Neurosci. *26*, 1767–1775.

Park, T.J., Hamanaka, H., Ohshima, T., Watanabe, N., Mikoshiba, K., and Nukina, N. (2003). Inhibition of ubiquitin ligase Siah-1A by disabled-1. Biochem. Biophys. Res. Commun. *302*, 671–678.

Pramatarova, A., Ochalski, P.G., Chen, K., Gropman, A., Myers, S., Min, K.T., and Howell, B.W. (2003). Nck beta interacts with tyrosine-phosphorylated disabled 1 and redistributes in Reelin-stimulated neurons. Mol. Cell. Biol. *23*, 7210–7221.

Pramatarova, A., Chen, K., and Howell, B.W. (2008). A genetic interaction between the APP and Dab1 genes influences brain development. Mol. Cell. Neurosci. *37*, 178–186.

Pinto-Lord, M.C., and Caviness, V.S., Jr. (1979). Determinants of cell shape and orientation: a comparative Golgi analysis of cell-axon interrelationships in the developing neocortex of normal and reeler mice. J. Comp. Neurol. *187*, 49–69.

Pinto-Lord, M.C., Evrard, P., and Caviness, V.S., Jr. (1982). Obstructed neuronal migration along radial glial fibers in the neocortex of the reeler mouse: a Golgi-EM analysis. Brain Res. *256*, 379–393.

Rakic, P. (1988). Specification of cerebral cortical areas. Science *8*, 170–176.

Redmond, L., Oh, S.R., Hicks, C., Weinmaster, G., and Ghosh, A. (2000). Nuclear Notch1 signaling and the regulation of dendritic development. Nat. Neurosci. *3*, 30–40.

Rice, D.S., and Curran, T. (2001). Role of the Reelin signaling pathway in central nervous system development. Annu. Rev. Neurosci. *24*, 1005–1039.

Rice, D.S., Sheldon, M., D'Arcangelo, G., Nakajima, K., Goldowitz, D., and Curran, T. (1998). Disabled-1 acts downstream of Reelin in a signaling pathway that controls laminar organization in the mammalian brain. Development *125*, 3719–3729.

Sanada, K., Gupta, A., and Tsai, L.H. (2004). Disabled-1-regulated adhesion of migrating neurons to radial glial fiber contributes to neuronal positioning during early corticogenesis. Neuron *42*, 197–211.

Sarkisian, M.R., Bartley, C.M., Chi, H., Nakamura, F., Hashimoto-Torii, K., Torii, M., Flavell, R.A., and Rakic, P. (2006). MEKK4 signaling regulates filamin expression and neuronal migration. Neuron *52*, 789–801.

Sawamoto, K., Yamamoto, A., Kawaguchi, A., Yamaguchi, M., Mori, K., Goldman, S.A., and Okano, H. (2001). Direct isolation of committed neuronal progenitor cells from transgenic mice coexpressing spectrally distinct fluorescent proteins regulated by stage-specific neural promoters. J. Neurosci. Res. *65*, 220–227.

Šestan, N., Artavanis-Tsakonas, S., and Rakic, P. (1999). Contact-dependent inhibition of cortical neurite growth mediated by notch signaling. Science *286*, 741–746.

Sheldon, M., Rice, D.S., D'Arcangelo, G., Yoneshima, H., Nakajima, K., Mikoshiba, K., Howell, B.W., Cooper, J.A., Goldowitz, D., and Curran, T. (1997). Scrambler and yotari disrupt the disabled gene and produce a reeler-like phenotype in mice. Nature *389*, 730–733.

Soriano, E., and Del Rio, J.A. (2005). The cells of cajal-retzius: still a mystery one century after. Neuron *46*, 389–394.

Stolt, P.C., and Bock, H.H. (2006). Modulation of lipoprotein receptor functions by intracellular adaptor proteins. Cell. Signal. *18*, 1560–1571.

Suetsugu, S., Tezuka, T., Morimura, T., Hattori, M., Mikoshiba, K., Yamamoto, T., and Takenawa, T. (2004). Regulation of actin cytoskeleton by mDab1 through N-WASP and ubiquitination of mDab1. Biochem. J. *384*, 1–8.

Tabata, H., and Nakajima, K. (2002). Neurons tend to stop migration and differentiate along the cortical internal plexiform zones in the Reelin signal-deficient mice. J. Neurosci. Res. *69*, 723–730.

Tissir, F., and Goffinet, A.M. (2003). Reelin and brain development. Nat. Rev. Neurosci. *4*, 496–505.

Trommsdorff, M., Gotthardt, M., Hiesberger, T., Shelton, J., Stockinger, W., Nimpf, J., Hammer, R.E., Richardson, J.A., and Herz, J. (1999). Reeler/Disabled-like disruption of neuronal migration in knockout mice lacking the VLDL receptor and ApoE receptor 2. Cell *97*, 689–701.

Walsh, C.A., and Goffinet, A.M. (2000). Potential mechanisms of mutations that affect neuronal migration in man and mouse. Curr. Opin. Genet. Dev. *10*, 270–274.

Ware, M.L., Fox, J.W., Gonzalez, J.L., Davis, N.M., Lambert de Rouvroit, C., Russo, C.J., Chua, S.C., Jr., Goffinet, A.M., and Walsh, C.A. (1997). Aberrant splicing of a mouse disabled homolog, mdab1, in the scrambler mouse. Neuron *19*, 239–249.

Wu, G., Lyapina, S., Das, I., Li, J., Gurney, M., Pauley, A., Chui, I., Deshaies, R.J., and Kitajewski, J. (2001). SEL-10 is an inhibitor of notch signaling that targets notch for ubiquitin-mediated protein degradation. Mol. Cell. Biol. *21*, 7403–7415.

Yoon, K., and Gaiano, N. (2005). Notch signaling in the mammalian central nervous system: insights from mouse mutants. Nat. Neurosci. *8*, 709–715.

Yoon, K.J., Koo, B.K., Im, S.K., Jeong, H.W., Ghim, J., Kwon, M.C., Moon, J.S., Miyata, T., and Kong, Y.Y. (2008). Mind Bomb 1-Expressing Intermediate Progenitors Generate Notch Signaling to Maintain Radial Glial Cells. Neuron *58*, 519–531.

Zaki, M., Shehab, M., El-Aleem, A.A., Abdel-Salam, G., Koeller, H.B., Ilkin, Y., Ross, M.E., Dobyns, W.B., and Gleeson, J.G. (2007). Identification of a novel recessive RELN mutation using a homozygous balanced reciprocal translocation. Am. J. Med. Genet. A. *143A*, 939–944.